Identification of tuna protein-derived peptides as potent SARS-CoV-2 inhibitors *via* molecular docking and molecular dynamic simulation

Zhipeng Yu[a], Ruotong Kan[a], Huizhuo Ji[a], Sijia Wu[a], Wenzhu Zhao[a,*], David Shuian[b], Jingbo Liu[c], Jianrong Li[a,*]

[a] *College of Food Science and Engineering, Bohai University, Jinzhou 121013, PR China*
[b] *Institute of Drug Discovery Technology, Ningbo University, Ningbo 315211, PR China*
[c] *Lab of Nutrition and Functional Food, Jilin University, Changchun 130062, PR China*

ABSTRACT

The present study aimed to identify potential SARS-CoV-2 inhibitory peptides from tuna protein by virtual screening. The molecular docking was performed to elicit the interaction mechanism between targets (M^{pro} and ACE2) and peptides. As a result, a potential antiviral peptide EEAGGATAAQIEM (E-M) was identified. Molecular docking analysis revealed that E-M could interact with residues Thr190, Thr25, Thr26, Ala191, Leu50, Met165, Gln189, Glu166, His164, Cys145, Gly143, and Asn119 of M^{pro} via 11 conventional hydrogen bonds, 9 carbon hydrogen bonds, and one alkyl interaction. The formation of hydrogen bonds between peptide E-M and the residues Gly143 and Gln189 of M^{pro} may play important roles in inhibiting the activity of M^{pro}. Besides, E-M could bind with the residues His34, Phe28, Thr27, Ala36, Asp355, Glu37, Gln24, Ser19, Tyr83, and Tyr41 of ACE2. Hydrogen bonds and electrostatic interactions may play vital roles in blocking the receptor ACE2 binding with SARS-CoV-2.

1. Introduction

The rapid spread of the novel coronavirus (SARS-CoV-2) as a serious threat to the world public health is in dire need of finding nutritional supplements with potential SARS-CoV-2 inhibition effect (Munster, Koopmans, van Doremalen, van Riel, & de Wit, 2020). The main protease (M^{pro}, also called 3CLpro) in SARS-CoV-2 virus is a necessary therapeutic target, which together with papain-like proteases is required to process polyprotein translated from viral RNA and recognize specific cleavage sites (Dai & Zhang, 2020; Gurung et al., 2020). The structure of SARS-CoV-2 M^{pro} complex contains the natural inhibitor N3 (Yang et al., 2003). Therefore, inhibiting the activity of the SARS-CoV-2 M^{pro} enzyme would help to block viral replication (Anand, Palm, Mesters, Siddell, Ziebuhr, & Hilgenfeld, 2002). Since no human protease with the similar cleavage specificity are known, inhibitors are unlikely to be toxic (Zhang & Lin, 2020). It also has been confirmed that SARS-CoV-2 infects human host cells by an initial isolate of its spike glycoprotein (S) and the receptor angiotensin-converting enzyme 2 (ACE2) on human cells (Hoffmann et al., 2020; Tan & Aboulhosn, 2020). SARS-CoV-2 was supposed to use the ACE2 as receptor for virus entry into host cells (Kozhikhova, Shilovskiy, & Shatilov, 2020). Blocking the interaction between the S protein of SARS-CoV-2 and

receptor-binding domain (RBD) of cellular receptors ACE2 can prevent virus entry. Therefore, ACE2 is also an attractive target for the treatment of SARS-CoV-2.

To date, no specific antiviral drug and clinically effective vaccine are available for the prophylaxis or treatment of the highly virulent SARS-CoV-2 infections in humans. In this situation, protein as a nutritional supplementation may be a helpful approach to improve immunity against SARS-CoV-2. The protein macromolecules were degraded into amino acids and peptides by gastrointestinal enzymes (Yao, Luo, & Zhang, 2020). In addition, many previous studies reported antivirus peptides with long chain peptides, including anti-Japanese Encephalitis virus peptide P1 (TPDCTRWWCPLT) (Wei et al., 2020), anti-Respiratory syncytial virus anti-LTP (R8K4K2KAC) and SA-35 (MITH-GCYTRTRHKHKLKKTL) (Kozhikhova et al., 2020), and the anti-West Nile Virus Envelope Protein peptide P9 (CDVIALLACHLNT) (Bai et al., 2007). Currently, the peptides are the potential therapeutic agents for their selectivity, specificity, low levels of side effects, and predictable metabolism. A number of highly potent antiviral peptides, such as the anti-HIV C-peptide (SJ-2176) (Jiang, Lin, Strick, & Neurath, 1993) and enfuvirtide (Lazzarin et al., 2003), have been approved for use as antiviral drugs, indicating that antimicrobial peptides can be developed into safe and effective antiviral therapeutics and prophylactics. The

binding abilities of these peptides to M^pro and ACE2 were evaluated, and the peptides with high affinity to the two enzymes could be expected to have a little bit potential inhibition on SARS-CoV-2. Tuna is a high content of nutrition ingredients food, and is widely consumed as a part of modern human diets (He, Su, Sun-Waterhouse, Waterhouse, Zhao, & Liu, 2019). Furthermore, it has been found that tuna hydrolysates have many biological activities, especially, the inhibitory activity against angiotensin converting enzyme (ACE) (Lee, Qian, & Kim, 2010; Li, Wang, Zhang, Wang, Zhu, & Ma, 2015). The ACE inhibitors may have the potential to prevent and to treat the acute lung injury after SARS-COV-2 infection (Pati, Mahto, Padhi, & Panda, 2020; Zheng & Cao, 2020). So, tuna-derived peptides can be used as nutritional supplementation and have potential inhibition of SARS-CoV-2 activity.

Nowadays, isolating, purifying and identifying bioactive peptides from protein hydrolysate is time-consuming, however, the process can be simplified and accelerated by multistep virtual screening method and *in silico* gastrointestinal (GI) digestion (Vercruysse, Smagghe, Matsui, & Van Camp, 2008). Computer analysis of bioactive peptides released after food proteolysis is useful (Gangopadhyay et al., 2016). Molecular docking refers to docking peptides with the active center of targets in DS software, which generates the CDOCKER energy in the process. The CDOCKER energy values are a standard to predict the stability of peptides-targets connection. Lower CDOCKER-energy value revealed that ligand was more likely to bind with the receptor and achieve more favorable conformation. (Nongonierma, Mooney, Shields, & Fitzgerald, 2013). Many studies have confirmed the reliability of *in silico* screening methods, which can be regarded as valid alternatives to classic methods (Fu, Young, Løkke, Lametsch, Aluko, & Therkildsen, 2016; Yu, Dong, et al., 2020; Yu, Ji, et al., 2020; Zhao, Xue, & Yu, 2019).

The purpose of present study was to identify novel peptides for COVID-19 patients from tuna protein as nutritional supplementation. To facilitate the rapid discovery of this peptides, a combination strategy of *in silico* hydrolysis and molecular docking was performed to discover novel inhibitory peptides against M^pro and the host receptor ACE2. The potential mechanism of peptides with virus targets M^pro and ACE2 was explored by Discovery Studio (DS) 2017 R2 software. And molecular dynamic simulations (MD) was performed to determine the binding affinity of peptide with the main protease and ACE2 of SARS-CoV-2 at room temperature. This study will improve the physical condition of COVID-19 patients and provide a new strategy for the treatment of SARS-CoV-2.

2. Materials and methods

2.1. GI digestion of tuna protein

Pepsin (EC 3.4.23.1), Trypsin (EC 3.4.21.4), and Chymotrypsin (EC 3.4.21.1) are three typical enzymes in the gastrointestinal tract, which were chosen for proteolysis in the present study (Yu, Dong, et al., 2020). The amino acid sequence of tuna skeletal myosin heavy chain (Accession of NCBI: BAA12730.1) was chosen from the National Center for Biotechnology Information (NCBI) database (https://www.ncbi.nlm.nih.gov/). The program ExPASy PeptideCutter (https://web.expasy.org/peptide cutter/) (Zhao, Chen, Li, Xu, Shao, & Tu, 2016) could predict the cleavage sites of protease in a protein sequence (Hochstrasser, protein identification and analysis tools in the ExPASy server), which was used to hydrolyze tuna skeletal myosin protein. Subsequently, peptides with more than 2 amino acids were selected for the following virtual screening.

2.2. Molecular docking of peptides and M^pro of SARS-CoV-2

All peptides were docked to M^pro of SARS-CoV-2 using CDOCKER program in DS 2017 R2 software, aimed to screen the potential M^pro inhibitory peptides. The X-RAY diffraction structure of M^pro in complex

Table 1
Docking score and predicted solubility of successfully docked peptides with CDOCKER-energy values less than 102.18 kcal/mol.

Peptide	Docking score with M^pro	Solubility
EEAGGATAAQIEM	154.676 kcal/mol	GOOD
QAEEAEEQANTH	150.145 kcal/mol	GOOD
EEEQEAK	148.618 kcal/mol	GOOD
QTEEDK	132.888 kcal/mol	GOOD
EQDTSAH	132.832 kcal/mol	GOOD
EEAQER	131.632 kcal/mol	GOOD
QATESQK	129.159 kcal/mol	GOOD
EQTER	125.889 kcal/mol	GOOD
IDVER	124.963 kcal/mol	GOOD
IEEEIK	124.963 kcal/mol	GOOD
GADAIK	121.809 kcal/mol	GOOD
DDAVR	121.009 kcal/mol	GOOD
VETEK	120.161 kcal/mol	GOOD
EEGQSE	120.042 kcal/mol	GOOD
TEIQTA	119.848 kcal/mol	GOOD
VDASER	118.695 kcal/mol	GOOD
EGAQK	117.485 kcal/mol	GOOD
QQEISD	117.262 kcal/mol	GOOD
QIEEK	117.232 kcal/mol	GOOD
QADSVAE	117.088 kcal/mol	GOOD
AITDAAM	116.956 kcal/mol	POOR
EAVAK	116.669 kcal/mol	GOOD
GEQIDN	115.839 kcal/mol	GOOD
NAEDK	114.26 kcal/mol	GOOD
QTENGE	112.528 kcal/mol	GOOD
QGEVED	111.960 kcal/mol	GOOD
EQIK	110.023 kcal/mol	GOOD
TQQIEE	109.476 kcal/mol	GOOD
EVSVK	109.195 kcal/mol	GOOD
DAEVR	108.908 kcal/mol	GOOD
SEVDR	107.165 kcal/mol	GOOD
EATSAS	106.675 kcal/mol	GOOD
TIEDQ	105.871 kcal/mol	GOOD
EEAK	105.193 kcal/mol	GOOD
ETDAIQR	104.486 kcal/mol	GOOD
VAEQE	103.805 kcal/mol	GOOD
EQVAM	103.438 kcal/mol	GOOD
AEIEE	103.407 kcal/mol	GOOD
DEAEA	103.111 kcal/mol	GOOD
NQIK	102.210 kcal/mol	GOOD

with inhibitor N3 was downloaded from the RCSB Protein Data Bank (PDB ID: 6LU7) (https://www.rcsb.org/), with the structure resolution of 2.16 Å (Jin et al., 2020). The inhibitor N3 and water molecules of M^pro were removed, and hydrogen atoms were added before docking by DS 2017 R2 software (Dassault Systemes Biovia, San Diego, CA, USA). The structure of the peptides was drawn by DS 2017 R2 software (Yu et al., 2018). The natural compounds (baicalin and baicalein) have shown the inhibitory activity of SARS-CoV-2 (Su et al., 2020a), which were downloaded from (https://pubchem.ncbi.nlm.nih.gov/). The ligands were minimized with CHARMm force field. Ligands and M^pro were docked by CDOCKER protocol of DS 2017 R2. The docking was carried out with coordinates x: −10.8, y: 12.5, z: 69.0, with a radius of 13.8 Å. The parameters were default. CDOCKER energy values of inhibitor N3 was given as the standard to select good predicted affinity peptides (calculated in kcal/mol).

2.3. Toxicity and solubility prediction of peptides

The peptide property calculator was used to predict the solubility of potential peptides, available at http://www.innovagen.com/ (Lafarga, O'Connor, & Hayes, 2015). Subsequently, the tool Quantitative Structure-Toxicity Relationship (QSTR) studies in DS 2017 was used to calculate the toxicity of selected peptides according to the important physico-chemical properties. Theory-Toxicity Prediction (TOPKAT) protocol in DS 2017 was used to predict four properties in toxicity, *i.e.,* Mutagenicity (Ames test), Developmental Toxicity Potential (DTP),
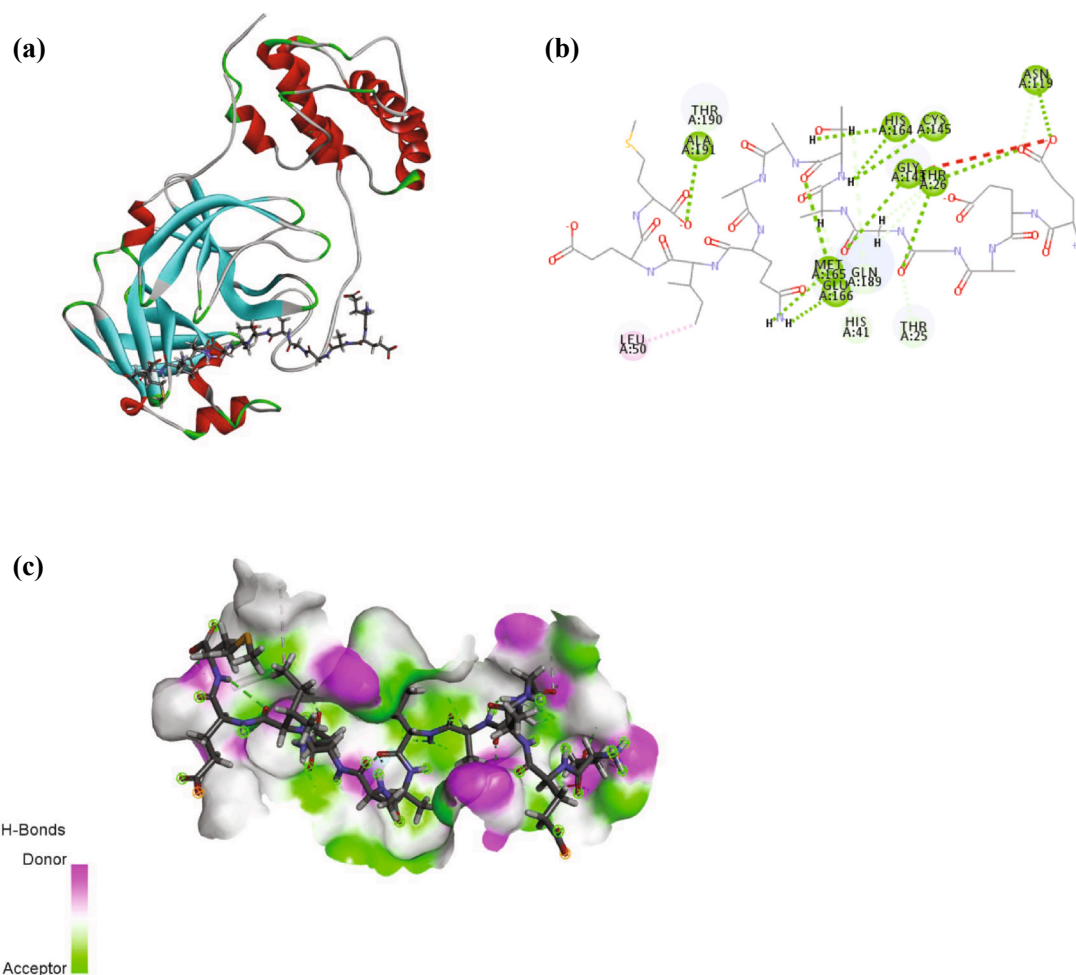
Fig. 1. The docking interactions of EEAGGATAAQIEM (E-M) with M^{pro} (PDB: 6LU7) and interactions with residues are shown in different colors. (a) 3D structure of peptide (E-M)-M^{pro} complex. (b) 2D diagram of the peptide (E-M)-M^{pro} molecular interactions. (c) The 3D hydrogen bonds surface plot at the binding site. The green color represents conventional hydrogen bond, light blue represents carbon hydrogen bond. The pink color represents alkyl interaction, and red color represents unfavorable acceptor–acceptor. (For interpretation of the references to color in this figure legend, the reader is referred to the web version of this article.)

Table 2
Docking with the amino acid residues of M^{pro}.

Ligand	Conventional hydrogen bonds	Carbon hydrogen bonds	Hydrophobic interaction
E-M	11	9	1
Inhibitor N3	8	6	2
Baicalin	5	2	5
Baicalein	–	–	3

("–": no interaction with the key amino acid residue).

Skin Sensitization (GPMT) and Rat Oral LD$_{50}$. TOPKAT protocol could accurately and rapidly evaluate the toxicity of peptides based on their 2D molecular structure.

2.4. Molecular docking of peptides and ACE2

The native crystal structure of the human ACE2 (PDB ID: 1R42) (Towler et al., 2004) was obtained from the PDB, with the resolution of 2.20 Å. Then, water molecules were removed and hydrogen atoms were added before docking. For docking simulations, a docking SBD site sphere was made to cover the entire two virus-binding hotspots of ACE2 (Wan, Shang, Graham, Baric, & Li, 2020), with coordinates x: 81.0, y: 76.5, z: 33.0, with a radius of 19.5 Å. And the CDOCKER program was used to molecular docking simulation in DS 2017. The potent binding

peptides to the ACE2 was selected based on the -CDOCKER-energy score.

2.5. Molecular dynamic (MD) simulation

MD simulations were carried out using GROMCS 2018 (Abraham et al., 2015) and the CHARMM36 force field (Brooks et al., 2009) for a period of 100 ns. A cubic box was built and the complex structures were placed in the center of the cubic box. Water molecules (TIP3P) were added to the remaining volume of the box, then each system was neutralized by adding chlorine/sodium atoms. The energy of each system was minimized by steepest descent algorithm (Dos Santos, Faria, Rodrigues, & Bello, 2020). To equilibrate the system, two step simulations (NVT and NPT) were carried out by leapfrog algorithm. NVT simulation was made for 1 ns using a V-rescale thermostat (Bussi, Donadio, & Parrinello, 2007) to keep the temperature at 300 K and NPT simulation was made for 1 ns using Berendsen barostat (Rogge et al., 2015) to maintain the pressure of each system at 1 bar. The simulation files were output to calculate the RMSD (Root Mean Square Deviation), RMSF (Root Mean Square Fluctuation) and Rg (radius of gyration) (Khan et al., 2020).
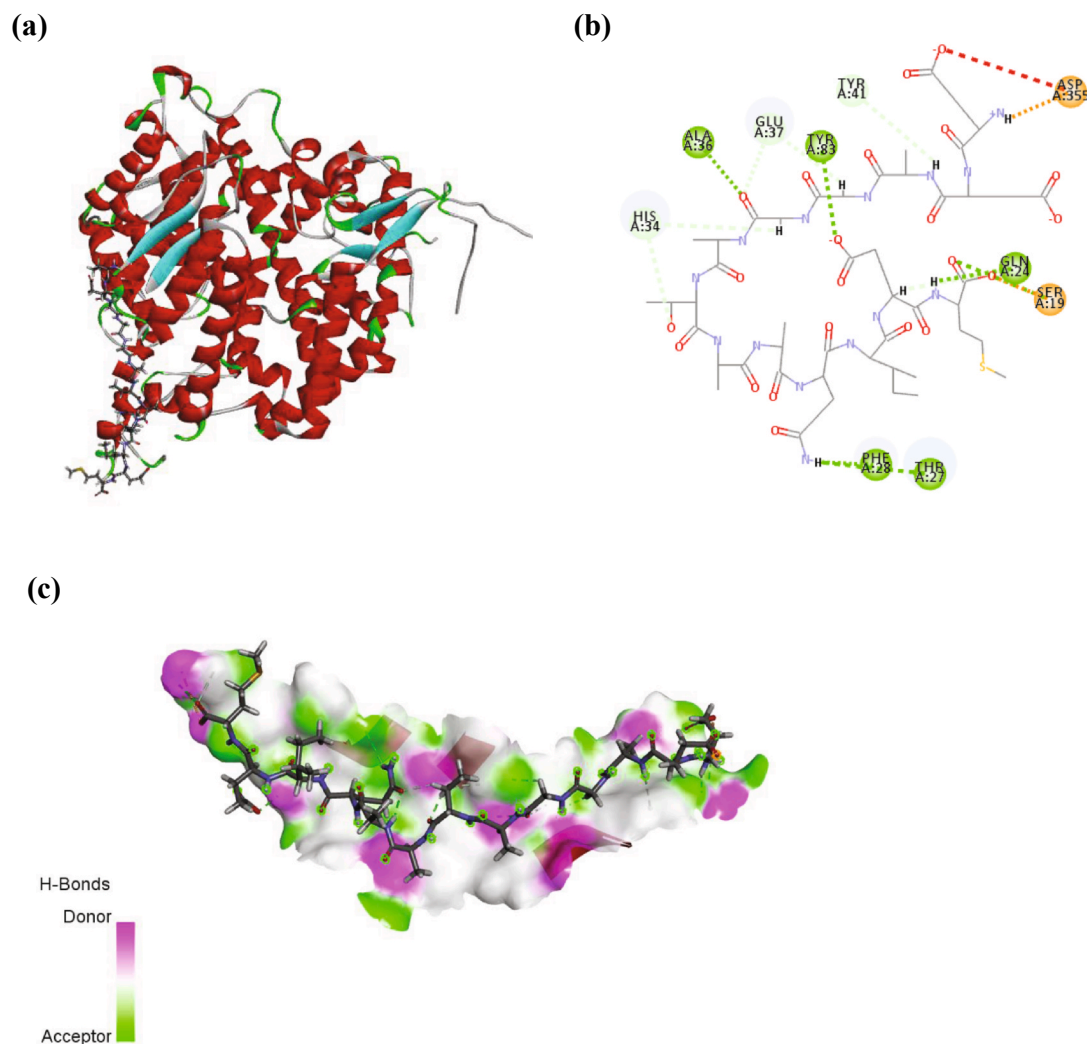
Fig. 2. The docking interactions of EEAGGATAAQIEM (E-M) with ACE2 (PDB: 1R42) and interactions with residues are shown in different colors. (a) 3D structure of peptide (E-M)-ACE2 complex. (b) 2D diagram of the peptide (E-M)-ACE2 molecular interactions. (c) The 3D hydrogen bonds surface plot at the binding site. The green color and light blue represent hydrogen bond. The orange represents electrostatic interaction, and red color represents unfavorable negative- negative. (For interpretation of the references to color in this figure legend, the reader is referred to the web version of this article.)

3. Results and discussions

3.1. Prediction M^{pro} inhibitory activity of peptides

A total of 142 peptides were obtained from skeletal myosin of tuna *in silico* digestion. *In silico* GI digestion, there are many challenges, such as, incomplete protein unfolding and hydrolysis of food proteins. In traditional digestion, it is hard to obtain high purity and potent active peptides with in complex mixtures of various peptides. Thus, there are differences between *in silico* GI digestion and real digestion. But compared with traditional digestion, in silico GI digestion is simpler, cost-effective, and faster. Subsequently, 136 peptides were successfully docked to M^{pro} of SARS-CoV-2 using CDOOCKER program in DS 2017 R2 software. The α-ketoamide inhibitor was a natural inhibitor similar to N3 inhibitor, which existed in the crystal structure of SARS-CoV-2 M^{pro} enzyme (PDB: 6Y2F) (Gurung, Ali, Lee, Farah, & Al-Anazi, 2020). The -CDOCKER-energy values of N3 inhibitor and α-ketoamide inhibitor were 102 and 50.3 kcal/mol, respectively. Compared with α-ketoamide inhibitor, N3 inhibitor had the lowest CDOCKER-energy. Therefore, 42 peptides with CDOCKER-energy values less than −102 kcal/mol were selected for following studies (shown in Table 1). Among the 42 peptides, peptide E-M had the lowest CDOCKER-energy, and it might have stronger binding affinity with the target M^{pro}. The

-CDOCKER-energy values of peptide E-M, baicalin and baicalein were 155, 19.5 and 30.0 kcal/mol, respectively. Compared with baicalin and baicalein which have been reported to have M^{pro} inhibitory activity (Su et al., 2020b), peptide E-M might have a better M^{pro} inhibitory activity.

3.2. Solubility, mutagenicity, toxicity properties predictions and docking with ACE2 of unknown peptides

The solubility results indicated that all these peptides were good water solubility except peptide AITDAAM (shown in Table 1). Water solubility of bioactive peptides plays a key role in the performance of physiological functions (Lee, Hong, Kim, & Lee, 2017). Peptides with good water solubility may have the potential of high biological availability. Thus, 41 peptides were selected to toxicity predictions. The evaluation of toxicity has an influence on the safety assessment of unidentified bioactive peptides, which directly related to the people's health. The TOPKAT mutagenicity and skin sensitization results showed that all peptides were Non-Mutagen and Non-Sensitizer (shown in Table 1). The Developmental Toxicity Potential results showed that peptides EEAQER, EEGQSE, QADSVAE, QGEVED, SEVDR and AVQSAR were toxic, others were Non-Toxic (shown in Table 1). The Rat oral LD50 value of all peptides were higher than that of etravirine (an anti-viral drug with LD50: 182.2 mg/Kg) (Singh et al., 2020), indicated that
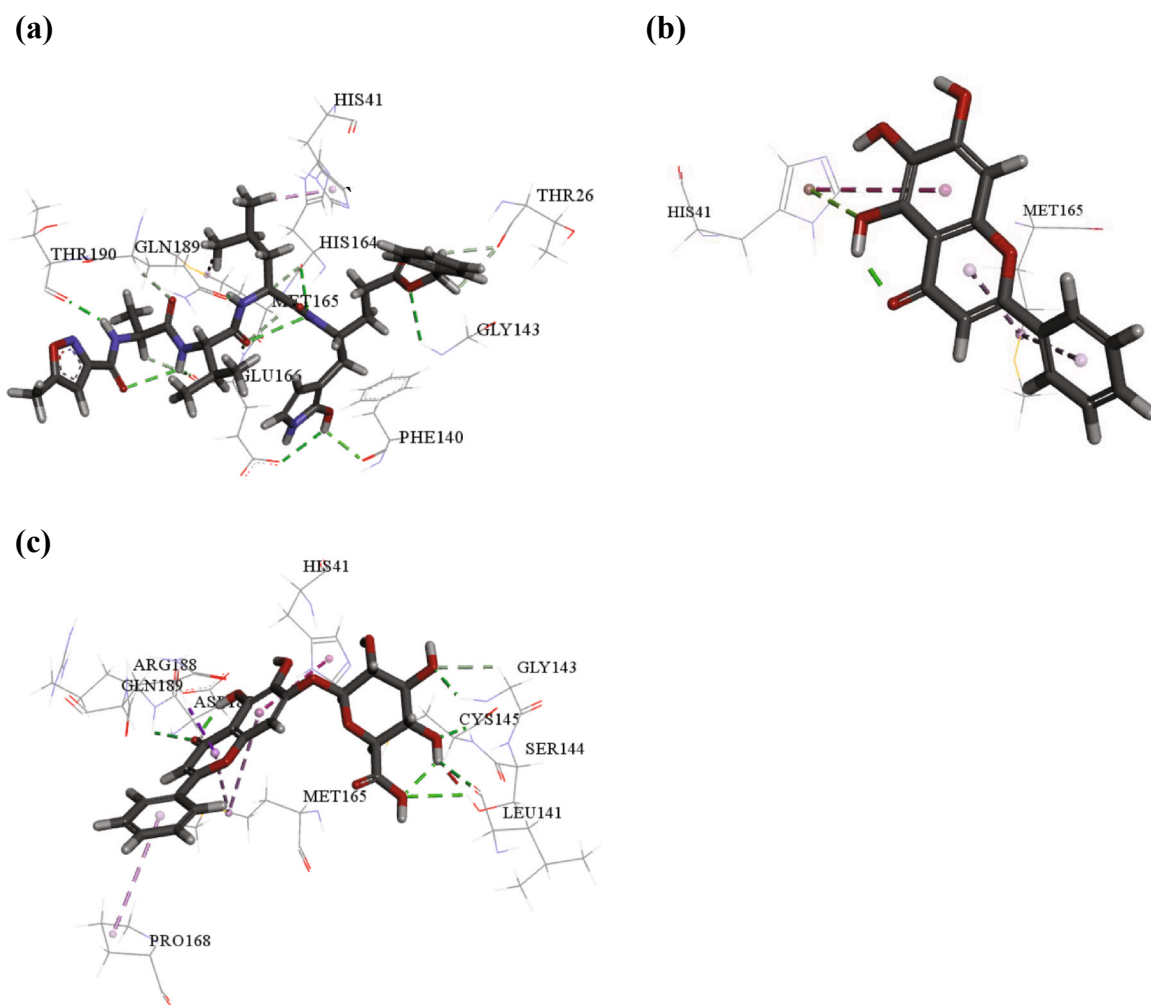
**Fig. 3.** Molecular interactions of inhibitor N3 (a), baicalein (b), and baicalin (c) into the M^{pro}.

the toxicity of all peptides may have a good safety index (shown in Table 1). In summary, 35 peptides with good water solubility, no-toxicity were subjected to the molecular dock to ACE2. Eventually, only one peptide EEAGGATAAQIEM (E-M) successfully docked with the virus host receptor ACE2. The -CDOCKER-energy value of the peptide E-M with ACE2 was 144 kcal/mol. Thus, the active site of ACE docked with SARS-CoV-2 spike was strongly occupied by peptide E-M, which could affect SARS-CoV-2 activity.

3.3. Molecular mechanism of potent SARS-CoV-2 inhibitory peptide E-M

In order to clarify the action mechanism of potential SARS-CoV-2 inhibitory peptides E-M with novel virus target M^{pro} and ACE2, molecular docking was performed. The best interaction posture of E-M with M^{pro} was stabilized by 11 conventional hydrogen bonds, 9 carbon hydrogen bonds, and 1 alkyl interaction (shown in Fig. 1). The residue Thr26 (HG1 and HN) of M^{pro} formed conventional hydrogen bonds with the atom O14 and O49 of E-M generating lengths 2.01 Å and 2.01 Å, respectively. The atoms H68 and H74 of E-M also formed two conventional hydrogen bonds with the residue His164 (O) of M^{pro} at distances 3.02 Å and 2.16 Å, respectively. The O80 and H114 of E-M formed conventional hydrogen bonds with HN and O of the residue Glu166 of M^{pro} at distances of 2.50 Å and 2.08 Å, respectively. Moreover, Asn119 (HN), Gly143 (HN) Cys145 (SG), Met165 (SD), and Ala191 (HN) of M^{pro} also formed conventional hydrogen bonds with atoms O15, O56, H68, H115 and O169 of E-M, at distances of 2.24 Å, 2.19 Å, 2.62 Å, 2.72 Å, and 2.02 Å, respectively. In the docked complex,

Asn119 (HA), Thr26 (O), Thr26 (O), Thr25 (HA), His41 (NE2), Met165 (HA), Gln189 (OE1), Thr190 (HB), and Gln189 (HA) formed carbon hydrogen bonds with O14, H54, H53, O49, H60, O80, H72, O169, and O112 of E-M at distances of 3.00 Å, 2.54 Å, 2.70 Å, 2.53 Å, 2.84 Å, 2.48 Å, 2.96 Å, 2.80 Å and 2.68 Å, respectively. Additionally, the residue Leu50 formed an alkyl interaction with E-M (C131) with a distance at 5.41 Å. Moreover, inhibitor N3 bound with residues Thr26, Gly143, Phe140, Glu166, Gln189, His164, His41, Thr190, and Met165 of M^{pro}, which were crucial residues for M^{pro} activity (shown in Fig. 3a). E-M formed interactions with M^{pro} by residues Thr190, Thr25, Thr26, Ala191, Leu50, Met165, Gln189, Glu166, His164, His41, Cys145, Gly143, and Asn119, part of which overlapped with the residues of inhibitor N3 action. As shown in Table 2, the total number of conventional hydrogen bonds and carbon hydrogen bonds in E-M was obviously more than N3 inhibitor, baicalin, and baicalein, indicating that the main interaction types of the complex were hydrogen bonds. The best docking postures of baicalein and baicalin with M^{pro} were shown in Fig. 3b, 3c. In the complex of baicalein-M^{pro}, the residues Met165, His41, Gly143, and Gln189 overlapped with the residues acted by the peptide E-M. Met165 and His41 mainly participate in hydrophobic interaction, and Gly143, and Gln189 mainly participate in the formation of hydrogen bonds. Compared with E-M, N3 inhibitor, and baicalein, this result was also confirmed. Therefore, hydrogen bonds between peptide and residues Gly143 and Gln189 of M^{pro} may be an important screening indicator.

The best posture of E-M binding with ACE2 (shown in Fig. 2) was stabilized by 6 conventional hydrogen bonds, 6 carbon hydrogen bonds,
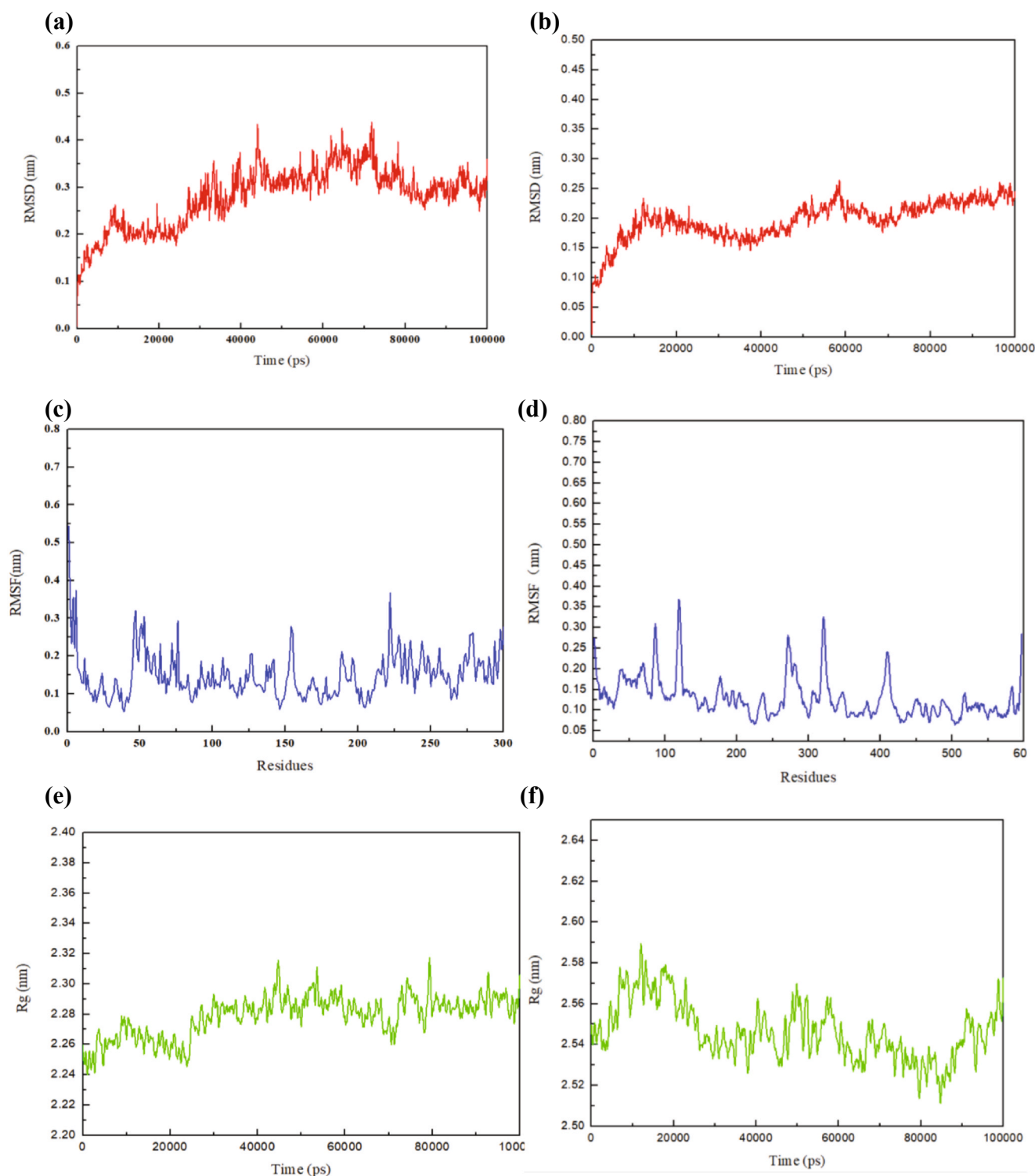
Fig. 4. The Root Mean Square Deviation (RMSD), Root Mean Square Fluctuation (RMSF) and radius of gyration (Rg) curves of the protein backbone (Cα) atoms during MD-simulation. RSMD (a), RMSF (c), and Rg (e) of M^{pro} in complex with peptide E-M. RSMD (b), RMSF (d), and Rg (f) of ACE2 in complex with peptide E-M. The complexes exhibited stable RMSDs, RMSFs and Rgs during a 100 ns MD simulation period.

1 pi-donor hydrogen bond, 1 salt bridge and 2 attractive charge interactions. The residues Ser19 (HT2), Gln24 (OE1), Tyr83 (HH), Phe28 (O) Thr27 (O) and Ala36 (HN2) of ACE2 formed conventional hydrogen bonds with the atoms O168, H153, O149, H114, H114 and O56 of E-M at distances of 2.98 Å, 2.01 Å, and 2.02 Å, 2.04 Å, 3.05 Å and 2.70 Å respectively. Glu37 (O), Glu37 (HC), His34 (O), His34 (HC), Gln24 (OE1), and Ser19 (HB1) formed carbon hydrogen bonds with the atoms

H46, O56, H54, O73, H140 and O168 of E-M at distances of 2.41 Å, and 2.43 Å, 2.59 Å, 2.40 Å, 3.00 Å and 2.88 Å respectively. Tyr41 of ACE2 formed a pi-donor hydrogen bond with E-M (H34) generating a length of 2.85 Å. Asp355 (OD1) of ACE2 formed a salt bridge with E-M (H4) generating a length of 2.10 Å. Two attractive charge interactions were observed in the complex (E-M)-ACE2, one involved the oxygen atom (OD1) of residue Asp355 with the hydrogen atom (H4) of E-M at a

6

distance of 2.10 Å, and the other one involved the nitrogen atom (N) of the residue Ser19 with the oxygen atom (O169) of E-M at a distance of 4.10 Å. In this study, peptide E-M bound with ACE2 by residues His34, Phe28, Thr27, Ala36, Asp355, Glu37, Gln24, Ser19, Tyr83, and Tyr41, among which His34, Phe28, Thr27, Ala36, Asp355, Gln24, Tyr83, and Tyr41 were demonstrated to involve in the interaction between viral spike and ACE2 (Ortega, Serrano, Pujol, & Rangel, 2020). Molecular docking results indicated that the formation of hydrogen bonds and electrostatic interactions might cause the committed interaction between the host receptor ACE2 and E-M. Additionally, it has reported that His34 of ACE2 is critical to bind with the pivotal residue Leu455 of SARS-CoV-2 spike protein (Ortega, Serrano, Pujol, & Rangel, 2020). In this study, carbon hydrogen bonds were formed between peptide E-M and the residue His34 of ACE2. These results indicated that peptide E-M may considered as potential inhibitor for SARS-CoV-2.

3.4. Molecular dynamic simulation studies

In order to get an idea about the structural stability, conformational fluctuations, compactness and folding behavior of M^{pro} complexed with peptide E-M and ACE2 complexed with peptide E-M, we performed MD simulations for 100 ns. The analysis of RMSD and RMSF usually provides important information about the stability and flexibility of the receptor-ligand complex. High deviation and fluctuation of proteins during a simulation may show weak stability (Ghosh & Chakraborty, 2020). SARS-CoV-2 M^{pro} in complexed with peptide E-M exhibited a stable RMSD between 0.25 nm and 0.4 nm (Fig. 4a) and the initial and final RMSDs during the whole simulation period were not found in the significance difference (0.2 nm and 0.3 nm). ACE2 in complexed with peptide E-M exhibited a stable RMSD between 0.15 nm and 0.25 nm (Fig. 4b) and the initial and final RMSDs during the whole simulation period were not found in the significance difference (0.1 nm and 0.2 nm). This showed a stable binding of peptide E-M with M^{pro} and ACE2. Moreover, residues fluctuations were also observed, not too flexible in motion. The residues fluctuation range in peptide E-M−M^{pro} complex is 0.053 nm-0.36 nm (Fig. 4c). The residues fluctuation range in peptide E-M−ACE2 complex is 0.075 nm-0.4 nm (Fig. 4d). Both, RMSD and RMSF stabilities were essential to infer good binding affinities (Doniach & Eastman, 1999; Dubey, Tiwari, & Ojha, 2013). Rg parameter was used to infer the degree of compactness and binding stability. A long range of variations in proteins show their weak folding. A steady value of Rg shows compactness and stable folding, which requires for proper function (Smilgies & Folta-Stogniew, 2015). On the contrary, in case of misfolding, the Rg will show a long range of variation over time (Lobanov, Bogatyreva, & Galzitskaia, 2008). The Rg values for peptide E-M-M^{pro} complexes were found to remain almost constant (2.27–2.29 nm) from 25 ns to 100 ns with some marginal fluctuations (Fig. 4e). The Rg values for peptide E-M-ACE2 complexes were found to remain almost constant, (2.52–2.58 nm) (Fig. 4f). The peptide E-M had good folding stability and high compactness with M^{pro} and ACE2. Thus, peptide E-M might be an effective inhibitor.

4. Conclusions

In this study, peptide E-M was identified from the skeletal myosin of tuna. Molecular docking simulation demonstrated that Gly143, and Gln189 played important roles in the interactions of peptide E-M and M^{pro}. Peptide E-M could block SARS-CoV-2 attachment to host cells by connecting with virus receptor ACE2 via hydrogen bonds and electrostatic interactions. Overall, peptide E-M has good safety due to their source of diet, and provide a good nutritional supplementation for COVID-19 patients. However, *ex vivo* and *in vivo* experiment will be required for further verify this conclusion. We want to share our results to anti- SARS-CoV-2 researchers as soon as possible, so we not do any further *in vivo* and *in vitro* experiments.

CRediT authorship contribution statement

Zhipeng Yu: Conceptualization, Methodology, Writing - review & editing, Supervision. **Ruotong Kan:** Data curation, Formal analysis, Writing - original draft. **Huizhuo Ji:** Visualization, Software. **Sijia Wu:** Writing - review & editing. **Wenzhu Zhao:** Software, Validation, Project administration. **David Shuian:** Supervision. **Jingbo Liu:** Investigation. **Jianrong Li:** Investigation, Validation.

Declaration of Competing Interest

The authors declare that they have no known competing financial interests or personal relationships that could have appeared to influence the work reported in this paper.

Appendix A. Supplementary data

Supplementary data to this article can be found online at https://doi.org/10.1016/j.foodchem.2020.128366.

References

Abraham, M. J., Murtola, T., Schulz, R., Páll, S., Smith, J. C., Hess, B., & Lindahl, E. (2015). GROMACS: High performance molecular simulations through multi-level parallelism from laptops to supercomputers. *SoftwareX, 1*.

Anand, K., Palm, G. J., Mesters, J. R., Siddell, S. G., Ziebuhr, J., & Hilgenfeld, R. (2002). Structure of coronavirus main proteinase reveals combination of a chymotrypsin fold with an extra alpha-helical domain. *EMBO Journal, 21*(13), 3213–3224.

Bai, F., Town, T., Pradhan, D., Cox, J., Ashish, Ledizet, M., et al. (2007). Antiviral peptides targeting the West Nile virus envelope protein. *Journal of Virology, 81*(4), 2047–2055.

Brooks, B. R., Brooks, C. L., III, Mackerell, A. D., Jr., Nilsson, L., Petrella, R. J., Roux, B., et al. (2009). CHARMM: The biomolecular simulation program. *Journal of Computational Chemistry, 30*(10), 1545–1614.

Bussi, G., Donadio, D., & Parrinello, M. (2007). Canonical sampling through velocity rescaling. *The Journal of Chemical Physics, 126*(1), 014101. https://doi.org/10.1063/1.2408420.

Dai, W., & Zhang, B. (2020). Structure-based design of antiviral drug candidates targeting the SARS-CoV-2 main protease. 368(6497), 1331-1335.

Doniach, S., & Eastman, P. (1999). Protein dynamics simulations from nanoseconds to microseconds. *Current Opinion in Structural Biology, 9*(2), 157–163.

Dos Santos, E. G., Faria, R. X., Rodrigues, C. R., & Bello, M. L. (2020). Molecular dynamic simulations of full-length human purinergic receptor subtype P2X7 bonded to potent inhibitors. *European Journal of Pharmaceutical Sciences, 152*, Article 105454.

Dubey, K. D., Tiwari, R. K., & Ojha, R. P. (2013). Recent advances in protein-ligand interactions: Molecular dynamics simulations and binding free energy. *Current Computer-Aided Drug Design, 9*(4), 518–531.

Fu, Y.u., Young, J. F., Løkke, M. M., Lametsch, R., Aluko, R. E., & Therkildsen, M. (2016). Revalorisation of bovine collagen as a potential precursor of angiotensin I-converting enzyme (ACE) inhibitory peptides based on in silico and in vitro protein digestions. *Journal of Functional Foods, 24*, 196–206.

Gangopadhyay, N., Wynne, K., O'Connor, P., Gallagher, E., Brunton, N. P., Rai, D. K., & Hayes, M. (2016). In silico and in vitro analyses of the angiotensin-I converting enzyme inhibitory activity of hydrolysates generated from crude barley (Hordeum vulgare) protein concentrates. *Food Chemistry, 203*, 367–374.

Ghosh, R., & Chakraborty, A. (2020). Identification of polyphenols from Broussonetia papyrifera as SARS CoV-2 main protease inhibitors using in silico docking and molecular dynamics simulation approaches. 1-14.

Gurung, A. B., Ali, M. A., Lee, J., Farah, M. A., & Al-Anazi, K. M. (2020). Unravelling lead antiviral phytochemicals for the inhibition of SARS-CoV-2 Mpro enzyme through in silico approach. *Life Sciences, 255*, 117831.

He, W., Su, G., Sun-Waterhouse, D., Waterhouse, G. I. N., Zhao, M., & Liu, Y. (2019). In vivo anti-hyperuricemic and xanthine oxidase inhibitory properties of tuna protein hydrolysates and its isolated fractions. *Food Chemistry, 272*, 453–461.

Hoffmann, M., Kleine-Weber, H., Schroeder, S., Krüger, N., Herrler, T., Erichsen, S., Schiergens, T. S., Herrler, G., Wu, N.-H., Nitsche, A., Müller, M. A., Drosten, C., & Pöhlmann, S. (2020). SARS-CoV-2 cell entry depends on ACE2 and TMPRSS2 and is blocked by a clinically proven protease inhibitor. *Cell, 181*(2), 271–280.e8.

Jiang, S. B., Lin, K., Strick, N., & Neurath, A. R. (1993). Inhibition of HIV-1 infection by a fusion domain binding peptide from the HIV-1 envelope glycoprotein GP41. *Biochemical and Biophysical Research Communications, 195*(2), 533–538.

Jin, Z., Du, X., Xu, Y., Deng, Y., Liu, M., Zhao, Y., et al. (2020). Structure of Mpro from COVID-19 virus and discovery of its inhibitors. *Nature, 582*, 1–9.

Khan, M. T., Ali, A., Wang, Q., Irfan, M., Khan, A., Zeb, M. T., Zhang, Y. J., Chinnasamy,

S., & Wei, D. Q. (2020). Marine natural compounds as potents inhibitors against the main protease of SARS-CoV-2-a molecular dynamic study. Journal of Biomolecular Structure and Dynamics, 1–11.

Kozhikhova, K. V., Shilovskiy, I. P., Shatilov, A. A., Timofeeva, A. V., Turetskiy, E. A., Vishniakova, L. I., et al. (2020). Linear and dendrimeric antiviral peptides: Design, chemical synthesis and activity against human respiratory syncytial virus. *Journal of Materials Chemistry B, 8*(13), 2607–2617.

Lafarga, T., O'Connor, P., & Hayes, M. (2015). In silico methods to identify meat-derived prolyl endopeptidase inhibitors. *Food Chemistry, 175*, 337–343.

Lazzarin, A., Clotet, B., Cooper, D., Reynes, J., Arastéh, K., Nelson, M., Katlama, C., Stellbrink, H.-J., Delfraissy, J.-F., Lange, J., Huson, L., DeMasi, R., Wat, C., Delehanty, J., Drobnes, C., & Salgo, M. (2003). Efficacy of enfuvirtide in patients infected with drug-resistant HIV-1 in Europe and Australia. *New England Journal of Medicine, 348*(22), 2186–2195.

Lee, J.-S., Hong, D. Y., Kim, E. S., & Lee, H. G. (2017). Improving the water solubility and antimicrobial activity of silymarin by nanoencapsulation. *Colloids and Surfaces B: Biointerfaces, 154*, 171–177.

Lee, S.-H., Qian, Z.-J., & Kim, S.-K. (2010). A novel angiotensin I converting enzyme inhibitory peptide from tuna frame protein hydrolysate and its antihypertensive effect in spontaneously hypertensive rats. *Food Chemistry, 118*(1), 96–102.

Li, Y., Wang, B., Zhang, H., Wang, Z., Zhu, S., & Ma, H. (2015). High-level expression of angiotensin converting enzyme inhibitory peptide Tuna AI as tandem multimer in Escherichia coli BL21 (DE3). *Process Biochemistry, 50*(4), 545–552.

Lobanov, M., Bogatyreva, N. S., & Galzitskaia, O. V. (2008). Radius of gyration is indicator of compactness of protein structure. *Molecular Biology (Mosk), 42*(4), 701–706.

Munster, V. J., Koopmans, M., van Doremalen, N., van Riel, D., & de Wit, E. (2020). A novel coronavirus emerging in china – key questions for impact assessment. *New England Journal of Medicine, 382*(8), 692–694.

Nongonierma, A. B., Mooney, C., Shields, D. C., & FitzGerald, R. J. (2013). Inhibition of dipeptidyl peptidase IV and xanthine oxidase by amino acids and dipeptides. *Food Chemistry, 141*(1), 644–653.

Ortega, J. T., Serrano, M. L., Pujol, F. H., & Rangel, H. R. (2020). Role of changes in SARS-CoV-2 spike protein in the interaction with the human ACE2 receptor: An in silico analysis. *EXCLI Journal, 19*, 410–417.

Pati, A., Mahto, H., Padhi, S., & Panda, A. K. (2020). ACE deletion allele is associated with susceptibility to SARS-CoV-2 infection and mortality rate: An epidemiological study in the Asian population. *Clinica Chimica Acta, 510*, 455–458.

Rogge, S. M. J., Vanduyfhuys, L., Ghysels, A., Waroquier, M., Verstraelen, T., Maurin, G., & Van Speybroeck, V. (2015). A comparison of barostats for the mechanical characterization of metal–organic frameworks. *Journal of Chemical Theory and Computation, 11*(12), 5583–5597.

Singh, V. K., Srivastava, R., Gupta, P. S. S., Naaz, F., Chaurasia, H., Mishra, R., & Rana, M. K. (2020). Anti-HIV potential of diarylpyrimidine derivatives as non-nucleoside reverse transcriptase inhibitors: design, synthesis, docking, TOPKAT analysis and molecular dynamics simulations. 1-17.

Smilgies, D. M., & Folta-Stogniew, E. (2015). Molecular weight-gyration radius relation of globular proteins: a comparison of light scattering, small-angle X-ray scattering and structure-based data. Journal of Applied Crystallography, 48(Pt 5), 1604-1606.

Su, H., Yao, S., Zhao, W., Li, M., Liu, J., Shang, W., et al. (2020a). Discovery of baicalin and baicalein as novel, natural product inhibitors of SARS-CoV-2 3CL protease < em > in vitro < /em > . bioRxiv, 2020.2004.2013.038687.

Su, H., Yao, S., Zhao, W., Li, M., Liu, J., Shang, W., et al. (2020b). Discovery of baicalin and baicalein as novel, natural product inhibitors of SARS-CoV-2 3CL protease in vitro.

Tan, W., & Aboulhosn, J. (2020). The cardiovascular burden of coronavirus disease 2019 (COVID-19) with a focus on congenital heart disease. *International Journal of Cardiology, 309*, 70–77.

Towler, P., Staker, B., Prasad, S. G., Menon, S., Tang, J., Parsons, T., et al. (2004). ACE2 X-ray structures reveal a large hinge-bending motion important for inhibitor binding and catalysis. *Journal of Biological Chemistry, 279*(17), 17996–18007.

Vercruysse, L., Smagghe, G., Matsui, T., & Van Camp, J. (2008). Purification and identification of an angiotensin I converting enzyme (ACE) inhibitory peptide from the gastrointestinal hydrolysate of the cotton leafworm, Spodoptera littoralis. *Process Biochemistry, 43*(8), 900–904.

Wan, Y., Shang, J., Graham, R., Baric, R. S., & Li, F. (2020). Receptor Recognition by the Novel Coronavirus from Wuhan: an Analysis Based on Decade-Long Structural Studies of SARS Coronavirus. Journal of Virology, 94(7).

Wei, J., Hameed, M., Wang, X., Zhang, J., Guo, S., Anwar, M. N., et al. (2020). Antiviral activity of phage display-selected peptides against Japanese encephalitis virus infection in vitro and in vivo. *Antiviral Research, 174*, 104673.

Yang, H., Yang, M., Ding, Y., Liu, Y., Lou, Z., Zhou, Z., et al. (2003). The crystal structures of severe acute respiratory syndrome virus main protease and its complex with an inhibitor. *Proceedings of the National Academy of Sciences, 100*(23), 13190–13195.

Yao, Y., Luo, Z., & Zhang, X. (2020). In silico evaluation of marine fish proteins as nutritional supplements for COVID-19 patients. *Food & Function, 11*(6), 5565–5572.

Yu, Z., Dong, W., Wu, S., Shen, J., Zhao, W., Ding, L., Liu, J., & Zheng, F. (2020). Identification of ovalbumin-derived peptides as multi-target inhibitors of AChE, BChE, and BACE1. *Journal of the Science of Food and Agriculture, 100*(6), 2648–2655.

Yu, Z., Ji, H., Shen, J., Kan, R., Zhao, W., Li, J., Ding, L., & Liu, J. (2020). Identification and molecular docking study of fish roe-derived peptides as potent BACE 1, AChE, and BChE inhibitors. *Food & Function, 11*(7), 6643–6651.

Yu, Z., Wu, S., Zhao, W., Ding, L., Fan, Y., Shiuan, D., Liu, J., & Chen, F. (2018). Anti-Alzheimers activity and molecular mechanism of albumin-derived peptides against AChE and BChE. *Food & Function, 9*(2), 1173–1178.

Zhang, L., & Lin, D. (2020). Crystal structure of SARS-CoV-2 main protease provides a basis for design of improved α-ketoamide inhibitors. 368(6489), 409-412.

Zhao, W., Xue, S., Yu, Z., Ding, L., Li, J., & Liu, J. (2019). Novel ACE inhibitors derived from soybean proteins using in silico and in vitro studies. *Journal of Food Biochemistry, 43*(9), e12975.

Zhao, Y., Chen, Z., Li, J., Xu, M., Shao, Y., & Tu, Y. (2016). Formation mechanism of ovalbumin gel induced by alkali. *Food Hydrocolloids, 61*, 390–398.

Zheng, H., & Cao, J. J. (2020). Angiotensin-converting enzyme gene polymorphism and severe lung injury in patients with coronavirus disease 2019. *The American Journal of Pathology, 190*(10), 2013–2017.